COMPARISON OF THE CALCULATED AND EXPERIMENTAL FATIGUE LIVES UNDER NON-PROPORTIONAL BENDING WITH TORSION OF 10HNAP STEEL

Z. Marciniak , D. Rozumek, E. Macha

Opole University of Technology, ul. Mikołajczyka 5, 45-271 Opole, Poland

Abstract The paper contains the results of fatigue tests of 10HNAP steel under non-proportional bending with torsion. The circular smooth specimens were tested. The tests were carried out at the fatigue test stands MZGS-200PL and MZGS-200L. The best results of experimental and calculation lives consistence for the considered materials was obtained using the criterion of maximum shear stresses in the critical plane and the Palmgren-Miner hypothesis of damage accumulation.

1. Introduction

Non-proportional loadings very often occur while service of machine elements [1]. In literature we can find many various fatigue failure criteria for description of material tests under multiaxial loading. Test results are described with stress [2], strain [3] and energy [4] criteria. The well known and often applied criteria were proposed by Gough and Pollard [5], McDiarmid [6], Papadopoulos [7], Brown and Miller [3], Macha [2]. Nishihara and Kawamoto [8] published the test results for four materials: two steels, cast iron and duralumin. Specimens were subjected to cyclic bending with torsion with different phase displacements between stresses and different ratios of stress amplitudes. In [9], Liu and Zenner were engaged in tests of non-proportional loading; they applied the criterion of shear stress intensity. Under bending with torsion they found that increase of the phase displacement between loadings from 0 to $\pi/2$ caused 20% drop of the strength limit for trapezoid-shaped loading, and 15% increase of the strength limit for triangular loadings.

The aim of this paper is comparison of the calculated and experimental fatigue lives obtained under proportional and non-proportional bending with torsion for 10HNAP steel.

2. Experiment

10HNAP steel was subjected to fatigue tests. The material is a low-alloy constructional steel. It is a general-purpose steel of higher resistance to atmospheric corrosion. Chemical composition and some mechanical properties of 10HNAP steel are presented in Tables 1 and 2.

Table 1. Chemical composition of 10HNAP steel in %

C	Mn	Si	P	S	Cr	Ni	Cu	Fe
0.11	0.52	0.26	0.098	0.016	0.65	0.35	0.26	Bal.

Table 2. Monotonic and fatigue mechanical properties of 10HNAP steel

σ_Y MPa	σ_U MPa	σ_{af} MPa	N_0 cycles	E GPa	ν
418	566	300	$3.1347 \cdot 10^6$	215	0.29

Specimens of round sections were tested (see Fig. 1) They were cut from the sheets 16 mm in thickness according to the rolling direction.

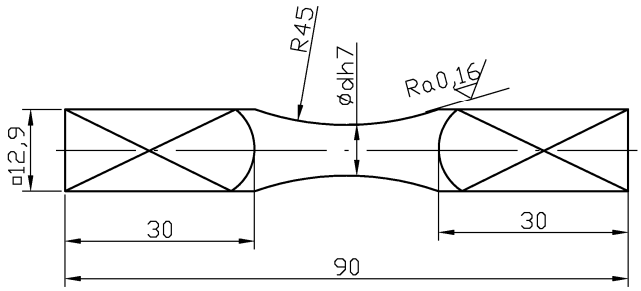

Fig. 1. Shape and dimensions of a specimen

The specimen surface was grinded and polished. Two diameters of the specimens were applied: d = 7.5 mm for variable-amplitude loading, and d = 8 mm for polyharmonic loading. The tests were realized at Opole University of Technology, at two fatigue tests stands: MZGS-200L (variable-amplitude loading) under frequency 20 Hz, and MZGS-200PL (polyharmonic loading); the dominating frequency was 29 Hz [10]. Fig. 2 shows the applied 30-second stress paths, registered during the tests. Figs. 2a and 2b show variable-amplitude stress paths registered under $\lambda_\sigma = 1$, and in Fig. 2c one can see polyharmonic stress paths for $\lambda_\sigma = 0.5$.

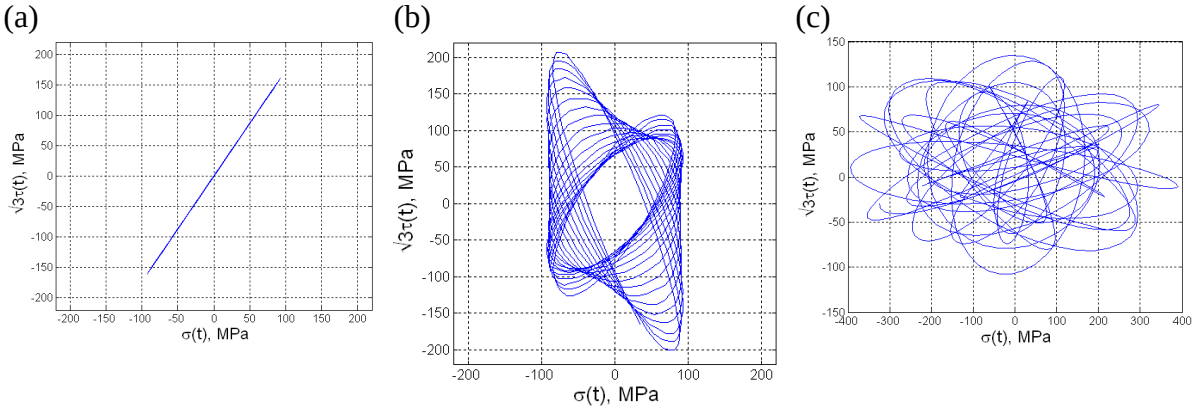

Fig. 2. Stress paths (a) proportional (variable-amplitude), (b) non-proportional (variable-amplitude), and (c) non-proportional (polyharmonic)

2.1. Procedure for fatigue life assessment

Fatigue life of the specimens was calculated according to the algorithm shown in Fig. 3. In the block 1 of the algorithm 820 s loading histories were registered during polyharmonic tests, and for variable-amplitude tests more than 2000 s loading histories were measured. Stresses were calculated using the elastic model of the material. In the block 2, the critical plane position was determined with the damage accumulation method The equivalent stress histories were calculated for the established position of the plane with the maximum damage degree (the block 3).

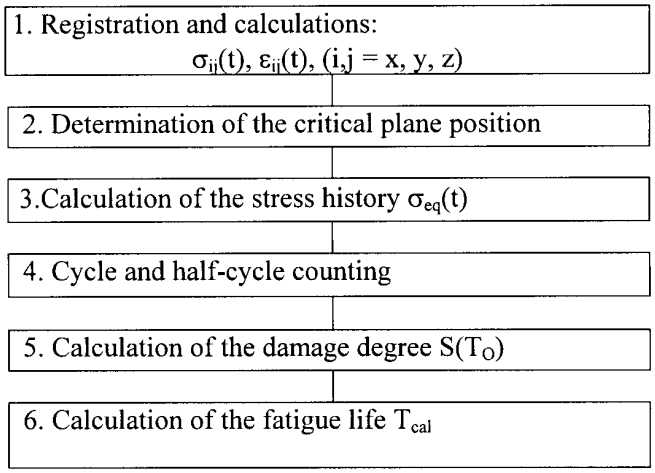

Fig. 3. A general algorithm of fatigue life calculations for materials under multiaxial service loading

The equivalent stress history $\sigma_{eq}(t)$ was calculated according to the following criteria [2]:
- criterion of the maximum shear stresses on the critical plane

$$\sigma_{eq}(t) = \sigma_x(t) \cdot \sin(2\alpha) + 2\tau_{xy}(t) \cdot \cos(2\alpha), \tag{1}$$

where α - the angle determining the critical plane position.
- criterion of the maximum normal stresses on the critical plane

$$\sigma_{eq}(t) = \sigma_x(t) \cdot \cos^2(\alpha) - \tau_{xy}(t)\sin(2\alpha) \tag{2}$$

- criterion of the maximum normal and shear stresses on the maximum shearing plane

$$\begin{aligned}\sigma_{eq}(t) &= (2-B)(\sigma_x(t) \cdot \cos^2(\alpha) - \tau_{xy}(t)\sin(2\alpha)) + \\ &+ B\left(-\frac{1}{2}\sigma_x(t)\sin(2\alpha) + \tau_{xy}(t)\cos(2\alpha)\right)\end{aligned}, \tag{3}$$

where:

$$B = \frac{\sigma_{-1}(N_f)}{\tau_{-1}(N_f)} \tag{4}$$

is the ratio of fatigue strength limits under bending and torsion for a number of cycles $N_f = 10^5$, assumed according to Sanetra [11]. Next, cycles and half-cycles were counted with the rain flow algorithm, and a damage degree $S(T_0)$ was calculated with use of the Palmgren-Miner hypothesis of damage accumulation [12, 13]:

$$S_{PM}(T_0) = \begin{cases} \sum_{i=1}^{k} \dfrac{n_i}{N_0\left(\dfrac{\sigma_{af}}{\sigma_{eq,ai}}\right)^m}; & \text{for} \quad \sigma_{eq,ai} \geq a \cdot \sigma_{af} \\ 0; & \text{for} \quad \sigma_{eq,ai} < a \cdot \sigma_{af}, \end{cases} \tag{5}$$

where
$\sigma_{eq,ai}$ – amplitude of the equivalent stress,

m – coefficient of the Wöhler curve slope under bending,
σ_{af} – fatigue limit under bending,
N_0 – number of cycles corresponding to the fatigue limit σ_{af},
n_i – number of cycle with amplitude $\sigma_{eq,ai}$ determined from the stress history $\sigma_{eq}(t)$ at observation time T_0,
a – coefficient including amplitudes below the fatigue limit while fatigue damage accumulation (a = 0.5 was assumed),
k – number of intervals in the amplitude histogram.
Calculations were also done with hypotheses by Serensen – Kogayev [14] and Corten – Dolan [15], where significant differences between calculations and experimental results were observed. In order to neglect influence of the stress gradient, fatigue characteristics for alternating bending were used for calculations.
Fatigue life T_{cal} was calculated according to the following equation:

$$T_{cal} = \frac{T_0}{S_{PM}(T_0)}, \tag{6}$$

where T_0 – observation time.

3. The test results and their analysis

The tests were realized under combined bending with torsion for two ratios of nominal stresses, λ_σ = 0.5 and 1, and for different cross-correlation coefficients, $r_{\sigma\tau}$ = 0, 0.5 and 1, under variable-amplitude histories [10]. The coefficient of loading irregularity for bending and torsion was I = 1. The MATLAB program was used for generation of random signals; next the signals were subjected to digital filtration by a narrow-band filter. The dominating loading frequency was 20 Hz. The periods of loading repetition were equal to 2000 seconds.
Fatigue tests of specimens made of 10HNAP steel were tested under nine loading combinations (see Table 3). The mean experimental lives under different ratios of nominal stresses λ_σ and cross-correlation coefficients $r_{\sigma\tau}$ for both tested steels were compared in Fig. 4. From the comparison of experimental data it appears that the correlation coefficient $r_{\sigma\tau}$, stresses σ_{max} and the ratio of stresses λ_σ strongly influence the fatigue life. In 10HNAP steel, under non-proportional stresses for λ_σ = 1 the mean experimental life is 1.8 times greater, and for λ_σ = 0.5 it is 5.2 times greater in relation to proportional stresses. Polyharmonic tests were performed for thirteen combinations of non-proportional bending with torsion under the constant cross-correlation coefficient $r_{\sigma\tau}$ = 0.16 and different ratios of maximum stresses (Table 4).

Table 3. Nominal stresses under variable-amplitude bending with torsion in 10HNAP steel at the stand MZGS-200L

Combination of loading	σ_{max} MPa	τ_{max} MPa	$\lambda_\sigma = \frac{\tau_{max}}{\sigma_{max}}$	Standard deviation $\sqrt{\mu_\sigma}$ (MPa)	Standard deviation $\sqrt{\mu_\tau}$ (MPa)	Correlation coefficient $r_{\sigma\tau}$
KWL1	212	212	1.0	53.43	53.43	0
KWL2	212	212	1.0	53.43	53.43	1
KWL3	301	150	0.5	75.86	37.80	1
KWL4	342	171	0.5	86.19	43.09	0
KWL5	342	171	0.5	86.19	43.09	1
KWL6	212	212	1.0	53.43	53.43	0.5
KWL7	320	160	0.5	80.65	40.32	0.5
KWL8	384	192	0.5	109.75	55.24	0
KWL9	320	160	0.5	80.65	40.32	1

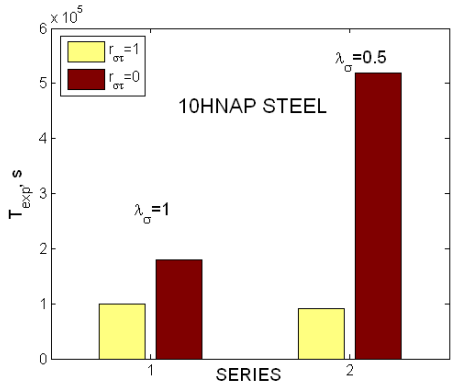

Fig. 4. Comparison of mean fatigue lives depending on different parameters of the stress state

Table 4. Nominal stresses under polyharmonic bending with torsion in 10HNAP steel at the stand MZGS-200PL

Combination of loading	σ_{max} MPa	τ_{max} MPa	$\lambda_\sigma = \frac{\tau_{max}}{\sigma_{max}}$	Standard deviation $\sqrt{\mu_\sigma}$ (MPa)	Standard deviation $\sqrt{\mu_\tau}$ (MPa)
K01	475	90	0.189	183.76	31.41
K02	475	130	0.274	185.32	47.74
K03	475	170	0.358	185.33	60.78
K04	475	210	0.442	182.51	74.04
K05	420	90	0.214	170.38	31.85
K06	420	130	0.309	159.20	49.65
K07	420	170	0.405	170.38	62.14
K08	420	210	0.500	168.25	82.08
K09	330	130	0.394	137.52	49.23
K10	330	170	0.515	133.96	62.14
K11	330	210	0.636	134.62	83.17
K12	250	170	0.68	96.25	57.55
K13	250	210	0.84	91.00	79.83

Power spectral density was characterized by four frequency peaks with the dominating peak 29 Hz. The coefficient of loading irregularity was I = 0.99 for bending and I = 0.97 for torsion. While testing, 820 s histories of bending and torsional moments were registered. They were applied for stress calculations in a linear-elastic range.

After calculations and considerations with the above methods it was found that the best life estimation was obtained according to the criterion of maximum shear stresses on the critical plane and the Palmgren-Miner hypothesis of damage accumulation. The comparison of the calculation and experimental results were presented in Fig. 5. From these figures it appears that:

(i) under variable-amplitude stress histories (Fig. 5a):

- for 10HNAP steel, 77 % of the results of fatigue life estimations are included into the scatter band with coefficient 2, and 100 % - into the scatter band with coefficient 3.

(ii) under polyharmonic stress histories (Fig. 5b):

- for 10HNAP steel, 73 % of the results of fatigue life estimation are included into the scatter band with coefficient 2, and 97% - into the scatter band with coefficient 3.

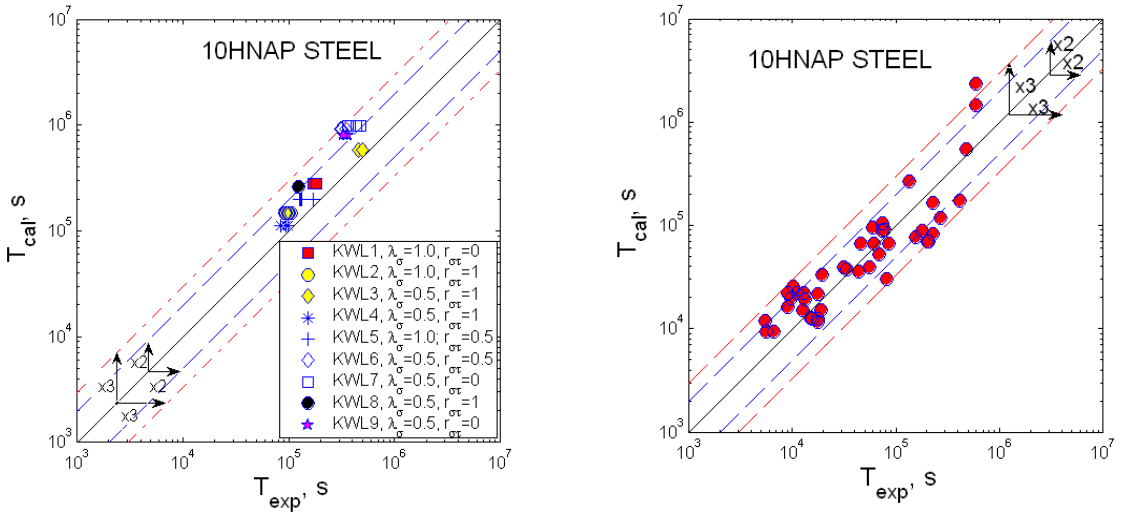

a) b)

Fig. 5. Comparison of the calculated lives T_{cal} with experimental ones T_{exp} for: a) variable-amplitude loading and b) polyharmonic loading

The results of life estimation according to the criterion of maximum normal stresses on the critical plane for variable-amplitude loading came out the scatter band with coefficient 3 and then the calculation life was overestimated. In the case of polymarmonic loading, 64 % of 10HNAP steel were included into the scatter band with coefficient 3. It can be found that according to the criterion of maximum normal and shear stresses on the plane of maximum shearing (variable-amplitude loading), 90 % of the results for 10HNAP steel are included into the scatter band with coefficient 3. In the case of polyharmonic loading, 97 % of 10HNAP steel were included into the scatter band with coefficient 3.

4. Conclusions

Basing on the calculated and experimental fatigue lives for the tested material, we can formulate the following conclusions:

1) The best agreement between the calculated and experimental results for variable-amplitude and polyharmonic loading was obtained according to the criterion of maximum shear stresses on the critical plane and the Palmgren-Miner damage accumulation hypothesis.
2) The considered criteria of maximum normal and shear stresses or normal stresses on the critical plane with use of the Palmgren-Miner damage accumulation hypothesis showed the overestimated calculation lives, exceeding the assumed scatter band with coefficient 3.
3) Application of damage cumulation hypotheses by Serensen-Kogayev and Corten-Dolan for all the considered criteria was not successful – significant divergence was observed.

References

1. Stephens R.I., Fatemi A., Stephens R.R., Fuchs H.O.: Metal Fatigue in Engineering, Second Edition, John Wiley & Sons, Inc., 2001, ps 472
2. Macha E.: Generalization of fatigue fracture criteria for multiaxial sinusoidal loadings in the range of random loadings, Biaxial and Multiaxial Fatigue, EGF 3, Eds M.W. Brown and K.J. Miller, Mechanical Engineering Publications, London 1989, pp. 425-436
3. Brown M.W., Miller K.J.: Two decades of progress in the assessment of multiaxial low-cycle fatigue life, in: Low-Cycle Fatigue and Life Prediction, Amzallag C., Leis B., Rabbe P., Eds ASTM STP 770, Philadelphia, 1982, pp. 482-499
4. Łagoda T., Macha E. & Niesłony A.: Comparison of the rain flow algorithm and the spectral method for fatigue life determination under uniaxial and multiaxial random loading, Journal of ASTM International, Vol. 1, No. 8, 2004, pp. 544-556
5. Gough H.J., Pollard H.V.: The effect of specimen form on the resistance of metals to combined alternating stresses, Proc. of the Institution of Mechanical Engineers, Vol. 135, 1935, pp. 549-573

6. McDiarmid D. L.: Fatigue behaviour under out-of-phase bending and torsion, The Aeronautical Journal of the Royal Aeronautical Society, March 1981, pp. 118-122
7. Papadopoulos I.V.: A new criterion of fatigue strength for out-of-phase bending and torsion of hard metals, Int. J. Fatigue, Vol. 16, 1994, pp. 377-384
8. Nishihara T., Kawamoto M.: The Strength of Metals under Combined Alternating Bending and Torsion with Phase Difference, Memoirs of the College of Engineering, Kyoto Imperial University, Vol. XI, No. 5, 1945, pp. 85-112
9. Liu J., Zenner H.: The fatigue limit of ductile metals under multiaxial loading, Biaxial/Multiaxial Fatigue and Fracture, ESIS 31, Eds A. Carpinteri, M. de Freitas and A. Spagnoli, Elsevier, London 2003, pp. 147-164
10. Marciniak Z.: Fatigue life of structural steels under non-proportional bending with torsion, Doctoral thesis, Opole University of Technology, 2005, p. 149 (in Polish)
11. Sanetra C.: Untersuchungen zum Festigkeitsverhalten bei mehrachsiger Randombeanspruchung unter Biegung und Torsion, Disseration, Technischen Universität Clausthal, Clausthal-Zellerfeld, 1991, s. 151
12. Palmgren A.: Die Labensdauer von Kugellagern, VDI-Z, Vol. 68, 1924, ss. 339-341
13. Miner M. A.: Cumulative damage in fatigue, Journal of Applied Mechanics Vol. 12, 1945
14. Serensen S.V., Kogayev V.P., Shnejderovich R.M.: Permissible loading and strength calculations of machine components, Third Edn., Mashinostroenie, Moskva 1975, 488 ps (in Russian)
15. Corten H. T., Dolan T. J.: Cumulative fatigue damage, Proc. of Int. Conf. on Fatigue of Metals, The Institution of Mechanical Engineers and ASME, London, New York 1956, pp. 235-246